MRS Communications (2017), 7, 84–89
© Materials Research Society, 2017
doi:10.1557/mrc.2017.9

MRS Communications

Research Letter

Selective laser melting of TiC/H13 steel bulk-form nanocomposites with variations in processing parameters

Bandar AlMangour, Franklin Yu, and **Jenn-Ming Yang,** Department of Materials Science and Engineering, University of California, Los Angeles, CA 90095, USA
Dariusz Grzesiak, Department of Mechanical Engineering and Mechatronics, West Pomeranian University of Technology, Szczecin, Poland
Address all correspondence to B. AlMangour at **balmangour@gmail.com**

(Received 7 October 2016; accepted 25 January 2017)

Abstract

TiC/H13 nanocomposite parts were processed by selective laser melting using various energy densities; one part also underwent hot isostatic pressing (HIP). The effect of energy density and HIPing on densification, microstructure, and hardness were evaluated. It was found that the densification was not largely affected by the energy density, but the HIP-treated sample displayed a large improvement in relative density. With increasing energy density, the microstructures showed high levels of dispersion of nanoparticles, while HIP treatment coarsened the microstructure and induced agglomeration. Both HIP treatment and increased energy density lowered hardness markedly; this was likely due to annealing effects.

Introduction

H13, a medium-carbon steel type, is commonly used for hot-work tooling such as drill bits, end mills, and utilize dies for punching, shearing, and forming materials; it is abundant in the industry.[1] H13 steel displays exceptional workability, good weldability, a low coefficient of thermal expansion, and resistance to oxidation and corrosion. Industry tools are often subjected to high loads that are applied quickly and in large temperature gradients; therefore, such tools must be able to withstand these conditions repeatedly without failure and significant deformation. For this reason, it is necessary to explore ways to strengthen and harden these tool steels in order to increase their longevity, save costs and increase efficiency.

One way to approach overcoming this challenge is by incorporating hard second-phase carbides into the steel matrix. Particulate-reinforced MMNC (metal matrix nanocomposites) have shown improved wear resistance, reduced cost, isotropic properties, and low density.[2,3] Since stable carbides coarsen more slowly than cementite, they have proven to be more effective at higher temperatures.[4] Adding TiC, which is thermodynamically stable in conjunction with the hard martensitic steel matrix, has shown increased stiffness, hardness, and wear resistance.[4–7] Conventional methods, however, such as casting or powder metallurgy, have displayed major flaws with their respective processing methods. These methods are often complex and time consuming, require costly molds, and can result in coarse grain structure.[8] Due to low working temperature, particle–matrix interfacial bonding is limited, and this may degrade the mechanical properties of the desired product.[9] Also, non-negligible Van der Waals attractive forces in metal–matrix composites (MMC) can result in an inhomogeneous microstructure.[10]

Additive manufacturing (AM) has shown to be an effective processing method for MMCs.[11,12] AM describes a process in which a product is formed incrementally, i.e., a layer-by-layer method. It uses computer-aided design (CAD) to fabricate three-dimensional metallic components.[13,14]. For the purposes of materials processing, such processes may prove significantly advantageous. Compared with traditional forms of processing, such as machining or powder metallurgy, AM does not exhibit a large cost upon fabricating complex objects; the process also takes less time and creates less waste, since only material that is necessary for the product is implemented.[15] One of the more promising AM processes is known as selective laser melting (SLM); with a high-energy laser beam, parts with high-density and complex structure may be formed through selective melting and solidification of loose metallic powder.[16,17] The high-energy density of the fiber laser beam in SLM processing induces an increase in temperature in the molten laser-induced pool while maintaining a relatively small melting pool and a rapid rate of cooling[18]; this is beneficial for obtaining parts with refined microstructure and better properties. The SLM can help to curb uncontrolled agglomeration of nanoparticles that lead to inhomogeneous microstructures and possibly the absence of favorable nanostructures.[8] In addition, the solidification rate of the powders eliminates phase segregation, which promotes better chemical homogeneity; this produces a fine microstructure with a uniform size distribution of carbides and nonmetallic inclusions,[19,20] increasing the high-edge toughness of the tools, which can lead to better cutting

https://doi.org/10.1557/mrc.2017.9 Published online by Cambridge University Press

performance in non-ideal conditions such as interrupted cutting, where the cutting edge may be subject to micro-chipping. Also, the AM process has a high degree of alloying flexibility, paving the way for the production of unique tool steels with special compositions that are unable to be formed with traditional casting methods due to problems with hot-workability and segregation.[21] Wear resistance, determined greatly by the content and distribution of carbides, is promoted by vanadium, molybdenum, and cobalt. AM processing is able to incorporate these elements in larger quantities than conventional methods without compromising other properties.

Unfortunately, a problem that arises in SLM processing is intermittent porosity in the product; to avoid this, one method that may be employed is hot isostatic pressing (HIP). The part is placed in a pressure vessel, where internal pressure and temperature are raised significantly. This process serves to remove major porosity and densify processed samples, and can form parts with relative densities of 90%–100%.[22]

To quantify the effect of laser energy input on the relative density, microstructure, and mechanical properties of the nanocomposite, the applied energy density of the laser must be scrutinized. Regarding these qualities, this work aims to establish a relationship between processing conditions, microstructural characteristics, and mechanical performance of TiC/H13 nanocomposites. In addition, the influence of HIP and its effects on microstructural and mechanical qualities will be quantified and analyzed.

Materials and methods

Commercially available gas-atomized H13 steel powder was employed to serve as the metal matrix, average 45 μm. TiC nanopowder was used as reinforcement; it was near-spherical and had a mean particle size of 50 nm. The powders were prepared by high-energy ball milling of H13 with 15% TiC powder. The milling process has been described in detail in the previous work.[4]

SLM parameters were fixed at: laser power (p), 100 W; spot size, 0.18 mm; hatch spacing (h), 0.12 mm, and layer thickness of the powder (d) was 0.05 mm. After, 8 h ball milled powder was deposited onto the substrate. The laser scanned the powder surface, following CAD data, using a "cross-hatching" scanning method. This process was repeated for each layer until 8×6 mm^2 cylindrical parts were formed. The applied volumetric energy density (VED) is defined by $E = (p/vhd)$,[18] where we control the value of E at 67, 100, 200, and 300 J/mm^3 by changing the scanning speed (v) and holding all other values constant.

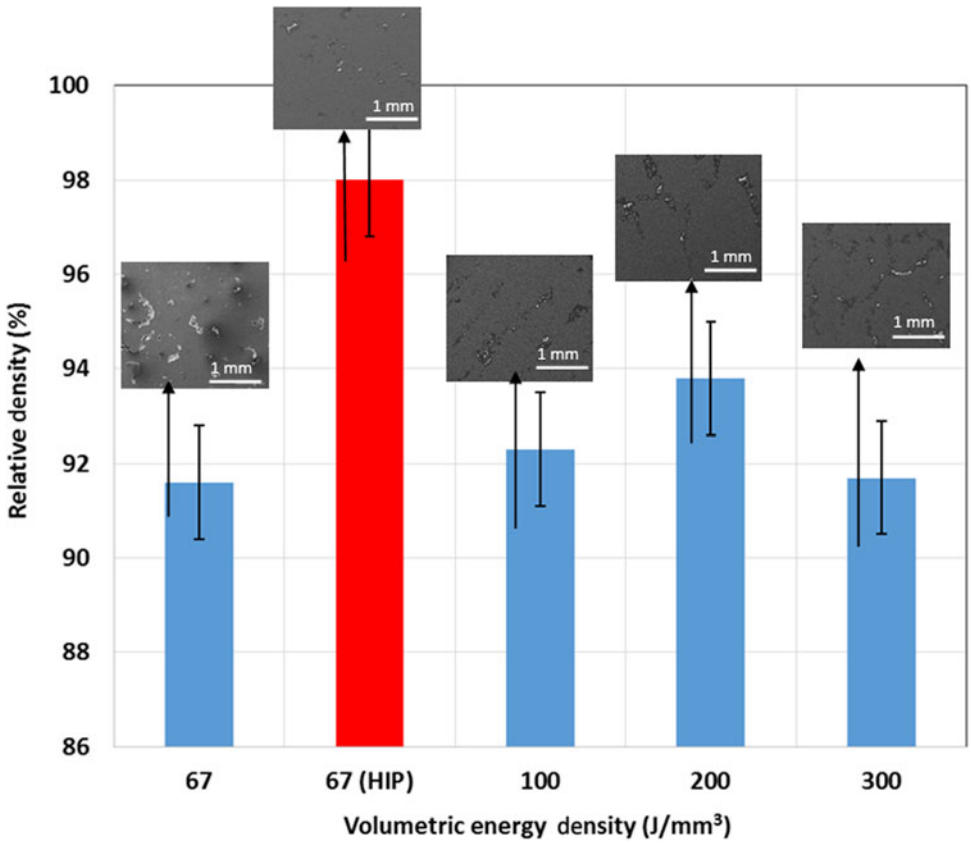


Figure 1. Effect of increasing VED on relative density of TiC/H13 nanocomposites. SEM images show change in morphologies at 50×. Also features effect of HIP on densification.

https://doi.org/10.1557/mrc.2017.9 Published online by Cambridge University Press

Afterward, standard HIP post-treatment was applied to the sample subject to the fastest scanning speed ($E = 67$ J/mm^3) using a service provided by Quintus Technologies, Ohio, USA. The samples were subject to HIP-treatment under a temperature of 1150 °C and pressure of 2070 bar using argon gas, and afterward rapid cooling was performed to 200 °C at a rate of 100 °C/min.

The viewed surfaces were ground and polished according to conventional metallographic procedures. Afterward, they were etched with a 3% Nital solution for 50 s. Later, the microstructures were observed using the Nova 230 scanning electron microscope (SEM).

Vickers hardness of the samples was measured with an LM800AT (Leco) tester at a load of 200 g and a dwell time of 10 s with a minimum of 15 indentations per sample.

Results and discussion

As shown in Fig. 1, the applied VED did not seem to markedly affect the densification. At $E = 67$ J/mm^3, the densification rate was 91.6%, and at the highest experimental VED value, where $E = 300$ J/mm^3, the densification rate was 91.7%. It is possible, due to restrictions in the quality of the equipment used, that the experimental conditions needed to be further optimized in order to see significant results; by changing another variable in addition to the scanning speed, such as power, we could expect to see a more noticeable change in the densification. Since the VED values used in this experiment were relatively low, the SLM temperature is restricted, leading to an increase of the melt viscosity.[23] Due to the material used and the relatively low VED, the wettability of the melt is decreased, possibly making densification more difficult to achieve.[24] Also,

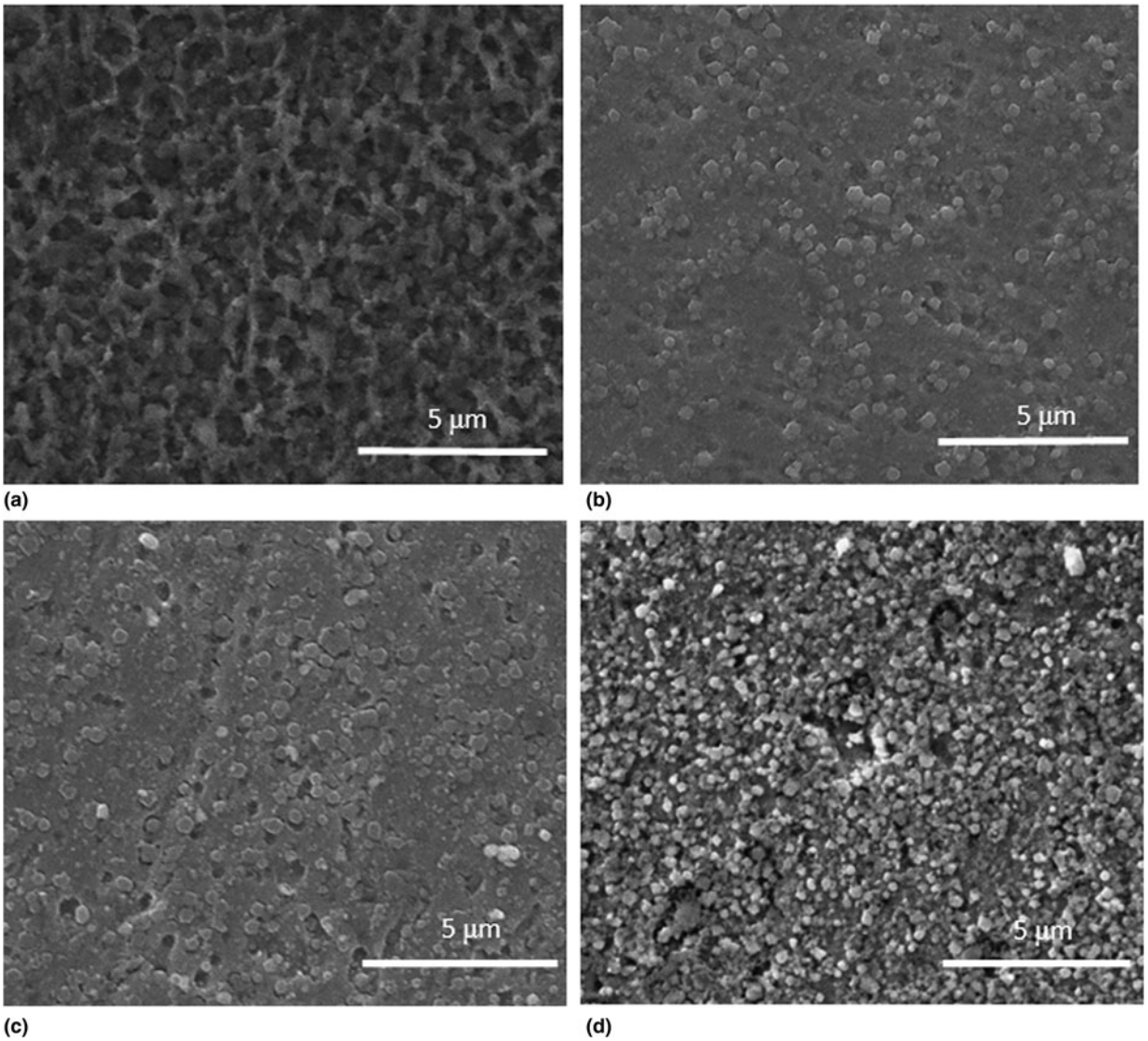


Figure 2. SEM images showing microstructural and dispersion states of TiC/H13 nanocomposites subject to SLM processing at varying VED: (a) $E = 67$ J/mm^3; (b) $E = 100$ J/mm^3; (c) $E = 200$ J/mm^3; (d) $E = 300$ J/mm^3.

https://doi.org/10.1557/mrc.2017.9 Published online by Cambridge University Press

when subject to laser scanning, the melting pool generates a temperature gradient between the center and the edge; this creates surface tension gradients and Marangoni flow, where the melt is inclined to flow radially toward the center.[25] As a result, the melt forms agglomerates; in conjunction with lower wettability, high viscosity, and high porosity, this hinders the densification of the nanocomposite samples.[26] However, despite the current conditions, we were able to see a large increase in densification upon hipping, as evident in Fig. 1. As a result of hipping conditions, plastic flow and particle shear occurs due to high temperature and pressure, leading to plastic deformation.[22] This serves to remove porosity and densify the sample. At the end of hipping densification, the isolated pores remaining are subject to bonding across the interface, where atoms diffuse both directions to close the pores.

Figure 2 displays the microstructural development of the samples with increasing VED upon etching. According to the SEM images, the TiC particle size is approximately 50–100 nm, a range similar to the initial size; it is, therefore, apparent that the applied energy density did not influence the particle size. However, further transmission electron microscope (TEM) characterizations are needed to properly analyze size distribution across varying energy densities. Contrarily, it is evident that the VED markedly affected the dispersion of the TiC. At lower VED, particles tend to gather into clusters, made of several nanoparticles. As the VED increased, the images showed that the TiC particles became more evenly distributed, and showed less signs of aggregation [Fig. 2(d)]. For moderately high temperatures, the laser heats and cools quickly, aiding the formation of TiC nanostructure by lessening the time required for TiC grains to grow. At these temperatures, the VED homogenizes the dispersion of the TiC nanoparticles. The higher SLM temperature, resulting from the high VED, increases the Marangoni flow in the melting pool and the magnitude of capillary force.[27] The Marangoni flow induces capillary forces for liquid flow,[28] and when it affects the TiC particles, a torque is applied around the particle because of its misalignment in the center.[25] This torque acts as a potential driving force for the nanoparticles to rearrange distribution in the sample.[29] As a result, the TiC particles have an increased rearrangement rate, and are inclined to cluster less and disperse more. Consequentially, at lower VED, the torque is reduced, and the particles tend to agglomerate.

Figure 3 displays a comparison between two samples subject to the same VED, the only difference being Fig. 3(b) has been HIP treated. Upon observation of the hipped sample, it is evident that the microstructure has coarsened significantly compared to the other sample. The particles have formed rough clusters, in contrast to pre-HIP microstructures. This phenomenon is likely due to the effects of annealing, which induces coarsening and coalescing mechanisms.[30] As expected, Fig. 3(b) also displays significantly less porosity, an additional testament to the recorded increase in densification.

Referring to previous works, we can see that the addition of TiC nanoparticles increased the Vickers hardness of H13 steel significantly, from 748.04 to 858.45.[6] Contrarily, in Fig. 4, the hardness values are shown with various VED values, and from the data shown, we see a large drop in microhardness from VED of 67 to 100 J/mm^3; the reason for this sudden reduction in hardness is grain growth resulting from elevated temperatures from the higher VED. However, as the VED increases further, the hardness plateaus. Similarly, upon hipping a sample exposed to a VED of 67 J/mm^3, we see a marked decrease in hardness. Despite the sample's increased densification, the hardness drops significantly upon hipping; this is likely due to the drastic change in microstructure from annealing effects

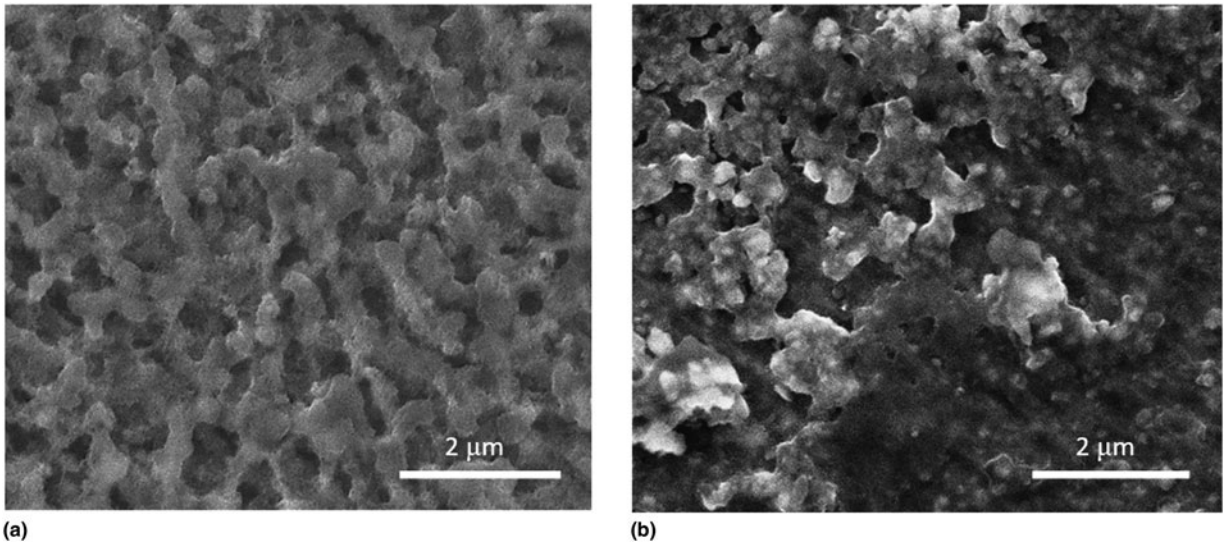


Figure 3. SEM images comparing non-HIP sample (a) to HIP sample (b) both subjected to SLM processing at VED of 67 J/mm^3.

https://doi.org/10.1557/mrc.2017.9 Published online by Cambridge University Press

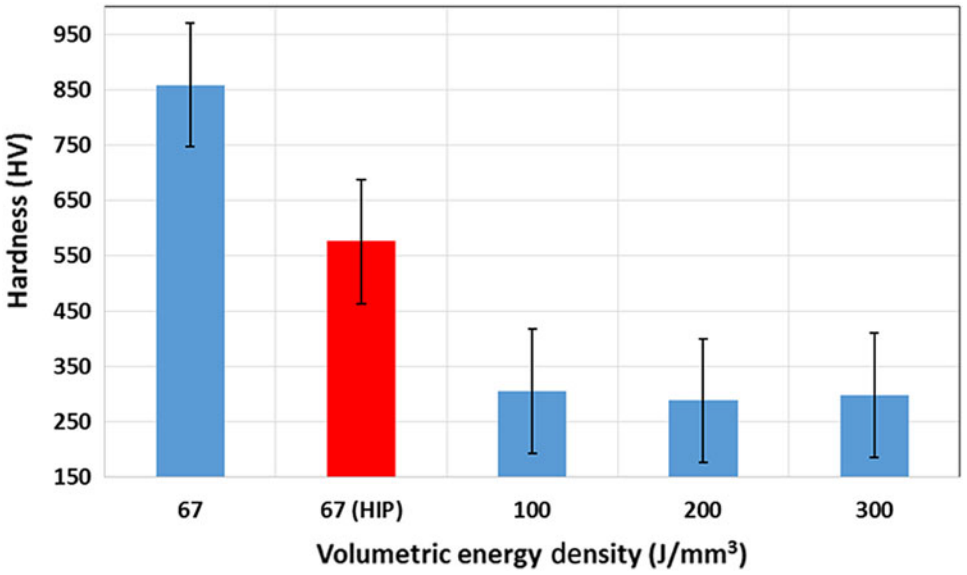


Figure 4. Effect of VED on Vickers hardness of TiC/H13 nanocomposite subject to SLM processing. Also displays effect of HIP treatment on microhardness.

under hipping conditions. The coarsening of the microstructure and the agglomerating of the particles likely has a larger effect on the hardness than the densification does, resulting in an overall decrease in hardness.[30]

Conclusion

In summary, the range of applied VED did not significantly affect the relative density of the nanocomposite samples; relatively low VED reduced the rate of densification due to high viscosity and porosity. In contrast, HIP treatment displayed a comparably large increase in densification, jumping from 91.6% to 98% relative density. By controlling the VED, the dispersion states of nanoscale TiC were altered; this played the largest role in determining the change in hardness for the nanocomposites. Despite the increased density due to HIP treatment, the hardness dropped due to the microstructural changes that occurred due to annealing effects, among them being coarsened grains and nanoparticle agglomeration. In addition, with increasing VED, the change in hardness followed in a similar fashion: under a VED of 67 J/mm^3, the hardness was recorded as 858.45, which dropped to 305.95 upon exposure to a VED of 100 J/mm^3.

Acknowledgments

One of the authors, Bandar AlMangour, gratefully acknowledges the financial support provided by the Saudi Arabia Basic Industries Corporation (SABIC).

References

1. J.F. Shackelford and W. Alexander: *CRC Materials Science and Engineering Handbook* (CRC Press, Boca Raton, FL, 2010).
2. I. Ibrahim, F. Mohamed, and E. Lavernia: Particulate reinforced metal matrix composites—a review. *J. Mater. Sci.* **26**, 1137–1156 (1991).
3. S.C. Tjong: Novel nanoparticle-reinforced metal matrix composites with enhanced mechanical properties. *Adv. Eng. Mater.* **9**, 639–652 (2007).
4. B. AlMangour, D. Grzesiak, and J-M. Yang: Nanocrystalline TiC-reinforced H13 steel matrix nanocomposites fabricated by selective laser melting. *Mater. Des.* **96**, 150–161 (2016).
5. E. Pagounis, V. Lindroos, and M. Talvitie: Influence of reinforcement volume fraction and size on the microstructure and abrasion wear resistance of hot isostatic pressed white iron matrix composites. *Metall. Mater. Trans. A* **27**, 4171–4181 (1996).
6. F. Akhtar: Microstructure evolution and wear properties of in situ synthesized TiB_2 and TiC reinforced steel matrix composites. *J. Alloys Compd.* **459**, 491–497 (2008).
7. W. Jiang, and P. Molian: Nanocrystalline TiC powder alloying and glazing of H13 steel using a CO_2 laser for improved life of die-casting dies. *Surf. Coat. Technol.* **135**, 139–149 (2001).
8. B. AlMangour, D. Grzesiak, and J-M. Yang: Selective laser melting of TiC reinforced 316L stainless steel matrix nanocomposites: influence of starting TiC particle size and volume content. *Mater. Des.* **104**, 141–151 (2016).
9. J. Hashim, L. Looney, and M. Hashmi: Particle distribution in cast metal matrix composites—Part I. *J. Mater. Process. Technol.* **123**, 251–257 (2002).
10. F. He, Q. Han, and M.J. Jackson: Nanoparticulate reinforced metal matrix nanocomposites-a review. *Int. J. Nanopart.* **1**, 301–309 (2008).
11. S. Kumar and J-P. Kruth: Composites by rapid prototyping technology. *Mater. Des.* **31**, 850–856 (2010).
12. D. Gu: *Laser Additive Manufacturing (AM): Classification, Processing Philosophy, and Metallurgical Mechanisms. Laser Additive Manufacturing of High-Performance Materials* (Springer, New York, 2015), pp. 15–71.
13. W.E. Frazier: Metal additive manufacturing: a review. *J. Mater. Eng. Perform.* **23**, 1917–1928 (2014).
14. I. Gibson, D. Rosen, and B. Stucker: *Additive Manufacturing Technologies: 3D Printing, Rapid Prototyping, and Direct Digital Manufacturing* (Springer, New York, 2014).
15. B. AlMangour and J-M. Yang: Improving the surface quality and mechanical properties by shot-peening of 17–4 stainless steel fabricated by additive manufacturing. *Mate. Des.* **110**, 914–924 (2016).
16. S. Bremen, W. Meiners, and A. Diatlov: Selective laser melting. *Laser Tech. J.* **9**, 33–38 (2012).
17. S.L. Campanelli, N. Contuzzi, A. Angelastro, and A.D. Ludovico: Capabilities and performances of the selective laser melting process. In

https://doi.org/10.1557/mrc.2017.9 Published online by Cambridge University Press

New Trends in Technologies: Devices, Computer, Communication and Industrial Systems, edited by M. Joo Er (InTech, 2010). Available from http://www.intechopen.com/books/new-trends-in-technologies–devices computer–communication-and-industrial-systems/capabilities-and-performances-of-the-selective-laser-melting-process
18. D. Gu, W. Meiners, K. Wissenbach, and R. Poprawe: Laser additive manufacturing of metallic components: materials, processes and mechanisms. *Int. Mater. Rev.* **57**, 133–164 (2012).
19. J-P. Kruth, P. Mercelis, J. Van Vaerenbergh, L. Froyen, and M. Rombouts: Binding mechanisms in selective laser sintering and selective laser melting. *Rapid Prototyping J.* **11**, 26–36 (2005).
20. M. Rombouts, J-P. Kruth, L. Froyen, and P. Mercelis: Fundamentals of selective laser melting of alloyed steel powders. *CIRP Ann. Manuf. Technol.* **55**, 187–192 (2006).
21. G. Roberts, G. Krauss, and R. Kennedy: *Tool Steels*, 5th ed. (ASM International, USA, 1998), p. 38.
22. H. Atkinson and S. Davies: Fundamental aspects of hot isostatic pressing: an overview. *Metall. Mater. Trans. A* **31**, 2981–3000 (2000).
23. A. Simchi and H. Pohl: Direct laser sintering of iron–graphite powder mixture. *Mater. Sci. Eng. A* **383**, 191–200 (2004).
24. Q. Jia and D. Gu: Selective laser melting additive manufacturing of TiC/Inconel 718 bulk-form nanocomposites: densification, microstructure, and performance. *J. Mater. Res.* **29**, 1960–1969 (2014).
25. H. Niu and I. Chang: Instability of scan tracks of selective laser sintering of high speed steel powder. *Scr. Mater.* **41**, 1229–1234 (1999).
26. D. Gu, Y-C. Hagedorn, W. Meiners, K. Wissenbach, and R. Poprawe: Nanocrystalline TiC reinforced Ti matrix bulk-form nanocomposites by Selective Laser Melting (SLM): densification, growth mechanism and wear behavior. *Composit. Sci. Technol.* **71**, 1612–1620 (2011).
27. M. Zhong and W. Liu: Laser surface cladding: the state of the art and challenges. *Proc. Inst. Mech. Eng. C: J. Mech. Eng. Sci.* **224**, 1041–1060 (2010).
28. J-P. Kruth, G. Levy, F. Klocke, and T. Childs: Consolidation phenomena in laser and powder-bed based layered manufacturing. *CIRP Ann. – Manufac. Technol.* **56**, 730–759 (2007).
29. D. Gu, H. Wang, D. Dai, P. Yuan, W. Meiners, and R. Poprawe: Rapid fabrication of Al-based bulk-form nanocomposites with novel reinforcement and enhanced performance by selective laser melting. *Scr. Mater.* **96**, 25–28 (2015).
30. S. Dadbakhsh and L. Hao: Effect of hot isostatic pressing (HIP) on Al composite parts made from laser consolidated Al/Fe 2 O 3 powder mixtures. *J. Mater. Process. Technol.* **212**, 2474–2483 (2012).

https://doi.org/10.1557/mrc.2017.9 Published online by Cambridge University Press